

The Overall Drag Losses For A Combination of Bodies

Dr. Sabah Jebour Al-Janabi

Material Engineering Dep. -Al- Mustansiriya University

Abstract

The objective of this work is to obtain better understanding of the flow over a combination of bluff bodies in close enough proximity to strongly interact with each other. This interaction is often beneficial in that the drag of the overall system is reduced. Proto-types for this problem come from tractor- trailer and missiles, and from various add-on devices designed to reduce their drag. Thus, an experimental investigation was carried out by placing conical frontal bodies having a base diameter of 0.65 cylinder diameter with different vertex angles (30°, 50°, 70°, and 90°). It was found that, the bluffer cone with 90° vertex angle gives the best minimum drag, which is 31% lower than the drag of the isolated cylinder. Also an interesting phenomenon was observed in that, the minimum drags for all combinations are obtained at the same gap ratio (i.e. at $g/d^2 = 0.365$).

Keywords: Drag loses, bluff bodies, fluid flow

الخسائر الاجمالية للكبح لمجموعة من الأجسام

الخلاصة

ان الغاية من هذا البحث هو للحصول على فهم افضل لحركة الموائع حول مجموعة من الاجسام غير الانسيابية والمتقاربة مع بعضها بما فيه الكافية، وتأثير احدهم على الاخر. ان هذا التأثير مفيد لانه يؤدي الى تقليل قوة الكبح الاجمالية للمجموعه. ان النموذج التجريبي لهذه المشكله بني على اساس التطبيقات العمليه والمستخدمه كما في القاطره والمقطوره والصواريخ والاستخدامات الاخرى .

لقد تم اجراء تجارب عمليه وذلك بوضع مخاريط اماميه اقطار قواعدها تساوي 65% من قطر الاسطوانه الخلفيه ولكن بزوايا رأسيه مختلفه (30,50,70,90) درجة وجد من التجارب بان المخروط الغير الانسيابي ذو الزاوية الراسية 90° اعطى افضل حد ادنى لقوه الكبح وهي 31% اقل من قوه كبح الاسطوانه المعزوله مقارنة ببقية المخاريط. اضافه الى ذلك تم ملاحظه ظاهره مثيره للانتباه وهي: ان الحد الادنى للكبح لكافه المجموعات قد حصل عند نسبه فجوه متساويه وهي 0.365.

الكلمات الدالة: قوة الدفع، الاجسام المسطحة ، جريان الموائع

Notations

C_D	Drag coefficient	R_D	Drags spring rate, N/ mm.
D	Drag force, N.	Re	Reynolds's number
d_1	Cone base diameter, mm.	RPD	Reference pressure difference, cm H ₂ O
d_2	Circular cylinder diameter, mm.	U_∞	Free air stream velocity, m/s.
g	Gap length ,mm.	μ	Air dynamic viscosity, Kg./ m s.
g/d_2	Gap ratio	ρ_a	Air density, Kg/m ³ .

Introduction

The drag forces of bodies in fluid flow are one of the most important problems and having a practical and theoretical interest for long time in many aerodynamic applications. Reduction of these forces is always required. Flow about bluff bodies, that is bodies on which pressure forces dominate due to large regions of stagnating and separating flow occurs in many practical situations and has been the subject of numerous applied studies through the years, for examples, in civil engineering the problem of drag losses in group of building ^[1] vibration of heat exchanger tubes in mechanical engineering, also the problem of the aerodynamic drag of tractor – trailer truck combinations ^[2,3].

Keith[4], investigated the shielding effects of various discs placed coaxially upstream of an asymmetric flat faced cylinder. Remarkable decrease of the drag of such system was observed for a certain gap ratio. Okajima^[5] clarified the flow characteristics of two circular cylinder in tandem arrangement for different Reynold's numbers, and found that, the drag coefficient of the upstream cylinder, varied with Reynold's number almost similar to those of single cylinders. The drag coefficient of the downstream cylinder changes with the variations of flow around the upstream cylinder, and the

spacing between them. Lee and Fowlar^[6], investigated the interference effect of a pair of square prisms on their mean lift and drag. They found that if the pair of prisms are placed parallel to the stream, the drag of the upstream prism is less than that of an isolated prism up to the gap size of 10d. Hossain^[7] measured the mean pressure distribution on a group of cylinders with square and rectangular cross sections in uniform cross flow, for various longitudinal spacing of the cylinders. He found that the drag coefficients on an isolated cylinder is higher in general that on the same cylinder while it becomes part of a group. Browand McArthur[8], recording the fuel consumption of two tandem trucks at spacing of 3,4,6,8 and 10 meters, found that, the average fuel consumption saving to be achieved by tandem operation varied from about 11% at 3-4 meters spacing to about 8% at 8-10 meter spacing.

A complete theoretical solution for the problem of flow over two bluff bodies in tandem has not yet been achieved, except for some simple cases. Thus the theoretical approach for the flow over tandem positioned bluff bodies could be considered from the following view points:

- 1- Flow separation and reattachment.
- 2- Recirculation of flow inside the gap.

The functional relationship for variation of drag around axis metric bluff bodies in tandem may be written as:

$$D = f(d_1, d_2, g, U_\infty, \rho, \mu) \dots\dots\dots (1)$$

Applying the dimensional analysis to above relations, Yield to;

$$C_D = f(R_e, d_1/d_2, g/d_2) \dots\dots\dots (2)$$

Where;

R_e is the Reynolds number

$$R_e = \rho \cdot U_\infty d_2 / \mu \dots\dots\dots (3)$$

The total drag on a body comprises of many elements; such as friction drag, pressure drag, and induced drag. Thus;

$$D = C_D \cdot \rho \cdot (U_\infty^2 / 2) \cdot A \dots\dots\dots (4)$$

The present investigation has been undertaken with the aim of gaining a better understanding of the fluid mechanics associated with the drag characteristics of conical frontal bodies having different vertex angles with a circular cylinder as a bluff body, and changing the spacing between them.

Experimental setup and procedure

All tests were carried out using an open type wind tunnel see (Fig.1-A), having a length of 4127 mm. The tunnel was constructed mainly of aluminum, the air is drawn into the tunnel through a diffuser by an axial fan unit, driven by 3-phase electric motor of 5kw power consumption. Different Reynolds's numbers were achieved at test section in the range of $1 \cdot 10^5$ to $2 \cdot 10^5$ (the Reynolds number was based on cylinder diameter) by means of double butterfly valve. The test section length is 1220mm and it is constructed from heavy gauge perspex material for clear visibility, having dimensions of 305 mm by 305 mm. The maximum air velocity could be obtained was about 36m/sec. For further description of this tunnel the reader should refer to the manufactures manual^[9].

The calibration factor (K) of the tunnel was obtained by the method described in reference^[10], and as follows: the reference pressure difference (RPD), was taken as the difference between the atmospheric pressure and the static pressure up stream of the testing model. The dynamic pressure was measured along the height of the testing section at different intervals in a plane near the static tapping, with different speeds.

The dynamic pressure is plotted against the reference pressure difference (Fig.1-B). The corresponding calibration factor was calculated from the figure, and it was found to be; $K=0.9357$, such that the average dynamic pressure (i.e., $1/2\rho u^2$), is equal to ($0.9357 \cdot RPD$).

Measurement of velocity distribution across the test section was taken at an interval of 1cm, and for different Reynolds numbers. The test results show the presence of a flat velocity profile with a boundary layer thickness of about 2cm near the walls, the results are shown in (Fig. 1-C).

The drag forces are measured, by means of a calibrated three component balance type (TE 81/ A) supplied with the tunnel. This balance is shown in (Fig. 1-D). The balance framework comprises of the base plate, which is screwed to the wind tunnel testing section by three studs, and carries a triangular force plate. These two plates are attached to each other, by a spherical universal joint, providing the balance with the necessary freedom.

The testing combination was mounted on the balance by means of a 12.7mm diameter steel stem. The air forces acting on the combination, and thus on the force plate are balanced by three springs of cantilever form, i. e (drag spring, and two lift springs), deflections of the drag spring and hence, drag forces are measured by means of a drag micrometer.

Every tested combination was mounted in the midpoint of the test section with zero incidence angle see (Fig. 1-E), and each test was carried out at various Reynolds number for each gap ratio. The accuracy of drag measurement is based on frequent calibration of drag instrument, i.e., the three -component balance, which means the accuracy of the micrometer and the drag dial gauge used for measuring the deflection of the drag spring, was within (± 0.1365) Newton. Figure (1 – F), represents the calibration curve of the drag parts of the balance. The spring rate is calculated from the slope of curve, and it was found to be equal to ($R_D=3.33$ N/mm).

The mean velocity of the free-stream was measured by means of a standard pitot-static tube of 4mm outside diameter located in the test section at a distance of (500) mm upstream of the test model; (Fig 1-G) shows its specifications. The pitot static leads were connected to a calibrated electrical micro manometer having a range of 0 to 100 mm water head. The air flow temperature was measured by means of thermal resistance probe .The accuracy of air velocity measurement was about (± 0.02) mm water.

The atmospheric pressure, air temperature, and relative humidity inside the testing room were measured by calibrated standard instruments.

Each test was performed for different Reynolds number; this was achieved by changing the mass flow rate passing the experimental model, by means of the butterfly valve. The flowing data were recording after achieving steady running condition:

- 1-Room temperature, atmospheric pressure, and relative humidity.
- 2-Total (stagnation) pressure head in mm water upstream the model.
- 3- Static heads up and down stream of the model in mm water.
- 4- The reading of drag micrometer in mm.
- 5-Free stream air temperature in °C.

Results and Discussion

The measurements are made in a wind tunnel whose test section is not large enough, and its solid wall does not duplicate exactly a free-stream (unbounded) environment, which contributes a constraining effect on the flow by making wall streamline, shaping makes the wall contours the wall contours, rather than being shaped by the flow field around the tested model. This effect and its magnitude have been the subject of many studies, one of best known is the analysis performed by Maskell[10] ,who developed a theory for pressure-drag correction for the effect of model blockage. The correction has the following form:

$$C_D/C_{DC} = 1 + \epsilon C_D B \dots\dots\dots(5)$$

Where;

- C_{DC} : corrected drag coefficient.
- ϵ : blockage factor =2.75 from Maskell ^[10].
- B: the ratio of model frontal area (cylinder base area) to the wind tunnel cross-sectional area.

Equation (5) above, was used to correct the blockage effect throughout this work.

A four cones having (30°, 50°, 70°, and 90°) vertex angles with a base diameter of 620mm each are placed in front of a circular cylinder (having 955mm diameter and 3820mm length) in tandem respectively. Thus four combinations were obtained for testing. From the above dimensions, the diameter ratio of cones to cylinder is equal to 0.65. Both cones and cylinder were made from aluminum alloys. . The base diameter of the cones were selected from patent by Sauners^[11],in which he found that a circular disc having a diameter of 0.65 to 0.75 cylinder diameter in tandem with circular cylinder are the best drag

reduction. The data for drag coefficient of isolated cones having vertex angles (30° , 50° , 70° , and 90°) were taken from Hoerner^[12].

Test results for combinations of bluff bodies were taken for Reynold's number ranging between, 1×10^5 and 2×10^5 .

Cone having 90° vertex angles:

The test results of this combination are presented in Figs (2, 3, 4 and 5). At gap-ratios (i.e., $g/d_2=0.05$, 0.1 , 0.15 , and 0.2), the drag coefficient of the combinations fluctuated between cylinder and cone values. Further increase in (g/d_2) causes a smooth reduction in drag coefficient reaching a minimum value of (0.65) at g/d_2 equal to (0.375), which is lower than the drag coefficient of the cylinder by 31%. Also it is lower than the value of the cone by 6.7%. For gap ratios in the range of 0.5 to 1.25, the drag coefficient starts to increase slightly above the minimum value obtained above, but still remained lower than the value of isolated cylinder, and lower than the drag coefficient of the isolated cone in some value at gap ratios.

For cone having 70° vertex angle

Gives a gradual reduction in drag coefficient associated with increasing g/d_2 as shown in Figs. (6 and 7), the optimum drag reduction for this combination was obtained at ($g/d_2=0.375$), where $C_D=0.64$, which similar to the value obtained in above combination.

50° vertex angle cone

The results of these combinations shown in Figs (8 and 9). The minimum value of drag coefficient occurred at ($g/d_2=0.375$), its average value is about 0.66. This value of drag coefficient is lower than the cylinder value, but is higher than the cone value.

30° vertex angle cone

Smooth decreasing in drag coefficient for this combination was

obtained at ($g/d_2=0.375$), see Figs. (10, 11, and 12). This reduction is about 19.5% lower than the drag coefficient of the cylinder, but it is higher than the values obtained in the fore mentioned combinations.

An interesting behavior is observed for the combinations of cones in tandem with the circular cylinder, when the drag coefficient is plotted against g/d_2 for $Re=2.0 \times 10^5$, as shown in Figs. (13 and 14). The most important features of these are; a smooth gradual reduction in drag coefficient associated with increasing gap length and up to $0.375d_2$, at which the optimum reduction is achieved, and this is true for all cones tested (i.e., cones having vertex angles 30° , 50° , 70° and 90°).

From these results, it is observed that, the greatest amount of drag reduction was achieved by the combination of cone having 90° vertex angle, relative to the other combinations tested. Fig. (15) shows the value of this reduction which is 20% lower than the value of the cone, if it is tested alone, and it is also lower by 31% than the value of drag coefficient for the cylinder if it is tested alone. The reason for this could be explained as follows; the bluffer cone (90°) tends to diverge the flow more, and the separated flow from the front body (cone) forms a thin, turbulent shear layer which joins tangentially onto the rear body (cylinder). This would be a well organized recirculation flow in gap between bodies by proper selected gap ratio. A consequence of this flow field is that the rear body face is exposed to pressures considerably below free stream static pressure. These low pressures, acting on the outer radial portions of the rear body face, balance the stagnation pressures on the front body face; and the resultant is a

reduction in drag forces of the combination.

Conclusions

- 1-Total drag of the cylinder is reduced for most of the combinations tested, the addition of the cones having vertex angles (30° , 50° , 70° and 90°) in front of the cylinder results in a 31% drag reduction, and it is worth emphasizing that, this is achieved by the bluffs cone, i.e.; cone having a 90° vertex angle.
- 2-This investigation leads to an important characteristic that, the optimum gap geometry, at which the minimum drag reduction was observed, is at gap ratio of 0.375 for all combinations tested.

References

1. Wise, A. F., "Effect due to group of building", Philosophical Transactions of the Royal Society of London, Series A, Vol.269, 1971, pp. 469-485.
2. Buckley, F. T. and Marks, C. h., "A wind- tunnel study of the effect of gap flow and gap seals on the aerodynamic drag of tractor- trailer trucks", T.A.S.M.E., Journal of Fluid Engineering, Vol. 100, December, 1978, pp. 434-438.
3. Chen, Y. N., "Frequency of the Karman vortex streets in tube Banks", Journal of the Royal aeronautical society, Vol.71, March, 1967, pp. 211-214.
4. Keith, K., A. Rosko, "An experimental Study of geometrical effect on the drag and flow of two bluff bodies separated by gap", J.Fluid Mech.(1985), Vol.156,pp.167-204 .
5. Okajima, A., "Flows around two tandem circular cylinders at very high Reynolds's numbers", Bulletin of the JSME, Vol.32, No. 166, April 1979,PP. 504-511.
6. Lee, B.E, and Fowler, G.R., "The mean wind force acting on a pair of square prisms ", Build Sci. Vol. 10,1975, PP. 107-110.
7. M. K. Hossain, M. Q. Islam, A.C. Mandal, and S. Saha", Wind effect on staggered cylinders of square and rectangular sections with variable longitudinal spacing", Journal of Mechanical Engineering, Vol. 1, ME38, Dec 2007.pp 52-57 Transactional the Mechanical Eng. Div., the Institution Engineering, Bangladesh.
8. Browand, J. Mc Arthur, and C. Radovich, "Fuel saving a achieved in the field test of tandem trucks" University of southern California, California PATH research report, UCS- ITS- PRR- 2004-250.
9. Plint and Partners ltd. 12 in *12 in. subsonic wind instruction manual. TE 54/A. England, 1980.
10. Maskell,E.C., " A theory of the blockage effects on bluff bodies and stalled wings in closed wind tunnel". Reports and Memoranda No.3400, November, 1963.
11. Sauners, W.S., "Apparatus for reducing linear and lateral wind resistance in a tractor – trailer combination Vehicle", U.S. Patent 4269444, No. 3241 876,2005.
12. Hoerner, S.F. "Fluid dynamic drag", Published by the author, Jan 1, 1965.by Amazon Com.U.S.A.

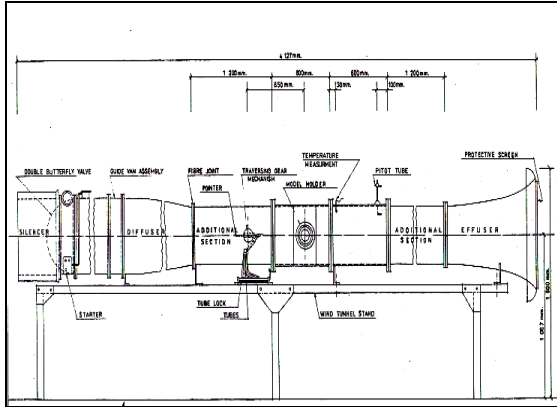


Fig. (1- A) Wind Tunnel

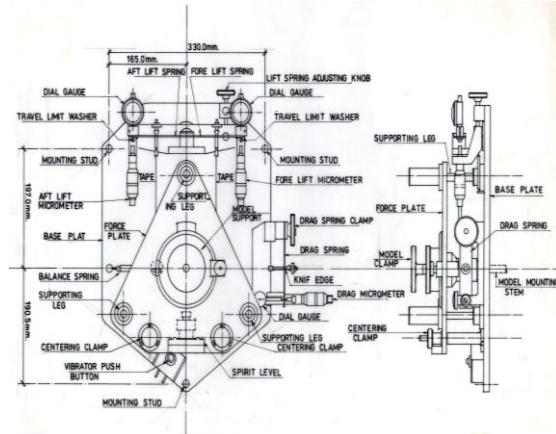


Fig. (1-D) Three – Component Balance

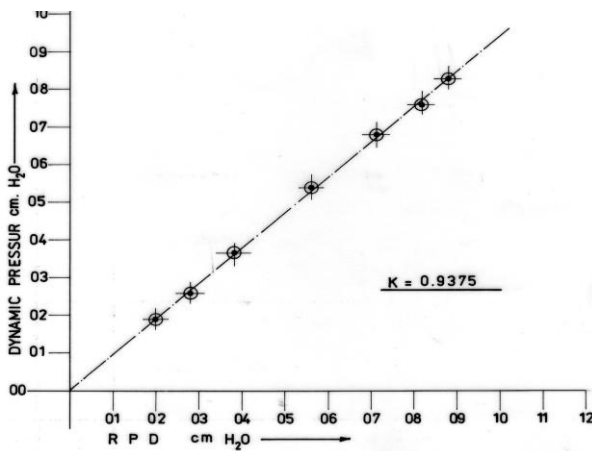


Fig.(1-B) Tunnel Calibration Curve

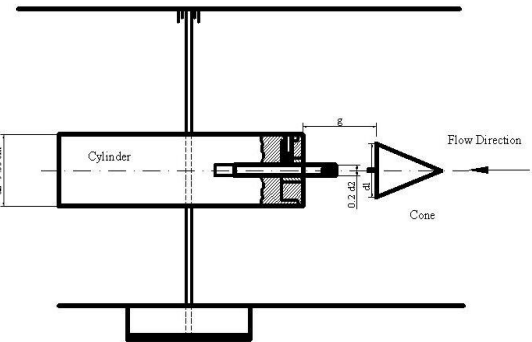


Fig. (1-E) Tested combination arguments.

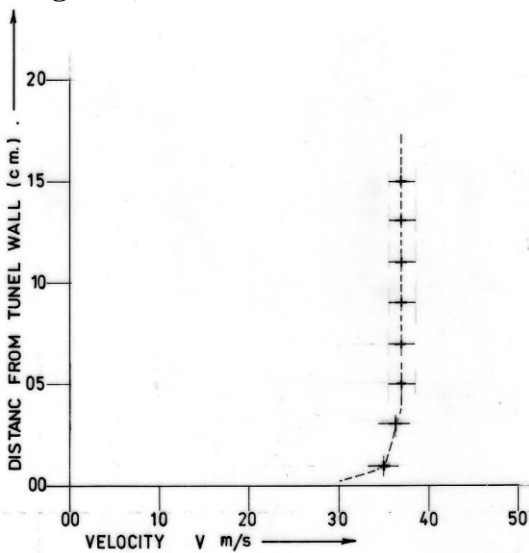


Fig.(1-C) Velocity Distribution in Test Section.

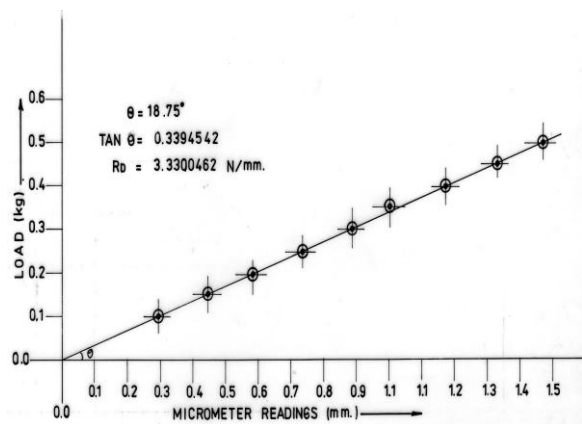


Fig.(1-F) Drag Spring Calibration Curve

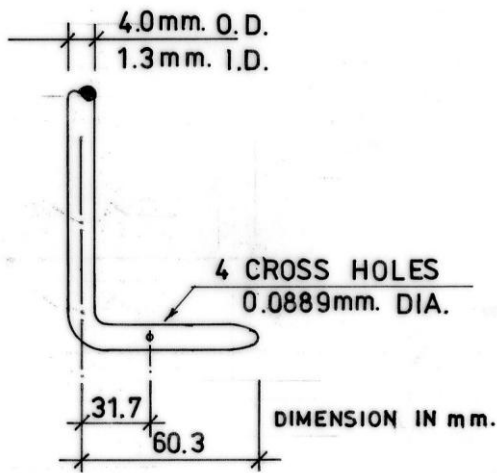


Fig. (1-H) Pitot – static tube

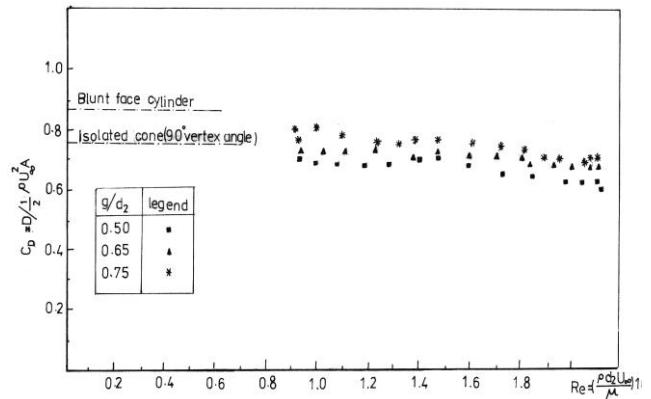


Fig.(4) Drag coefficient versus Reynolds number for a cone 90°vertex angle in tandem with the cylinder

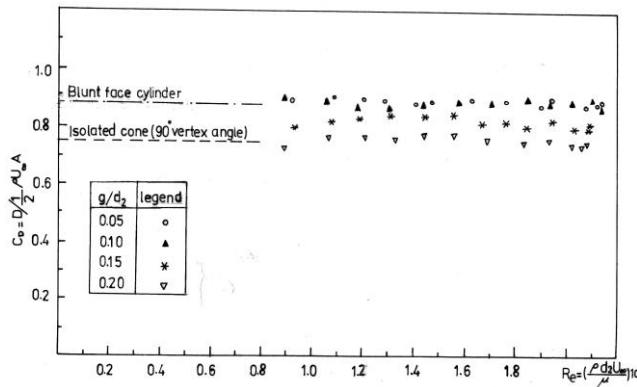


Fig.(2) Drag coefficient versus Reynolds number for a cone 90°vertex angle in tandem with the cylinder

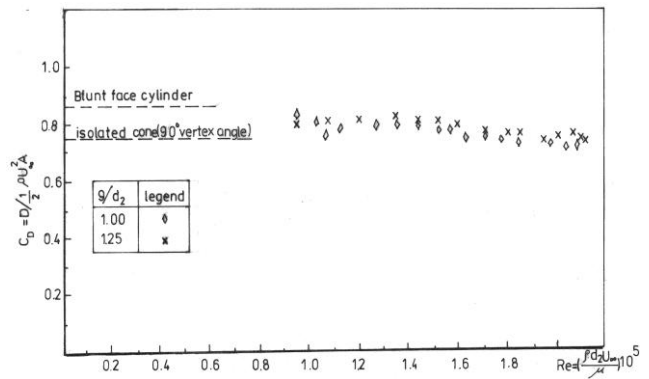


Fig.(5) Drag coefficient versus Reynolds number for a cone 90°vertex angle in tandem with the cylinder

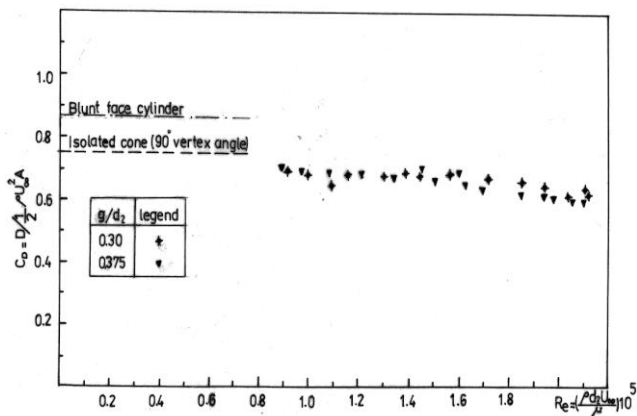


Fig.(3) Drag coefficient versus Reynolds number for a cone 90°vertex angle in tandem with the cylinder

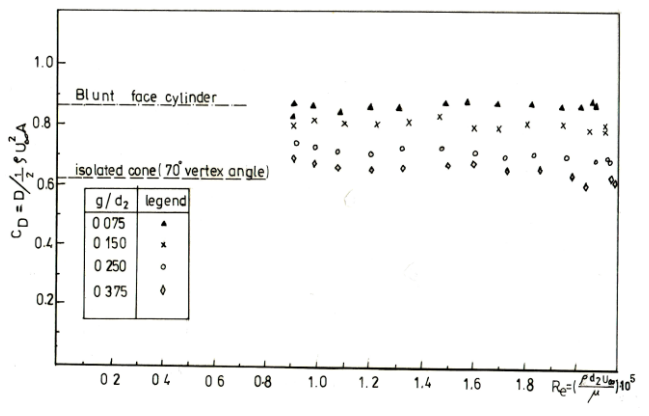


Fig.(6) Drag coefficient versus Reynolds number for a cone 70°vertex angle in tandem with the cylinder

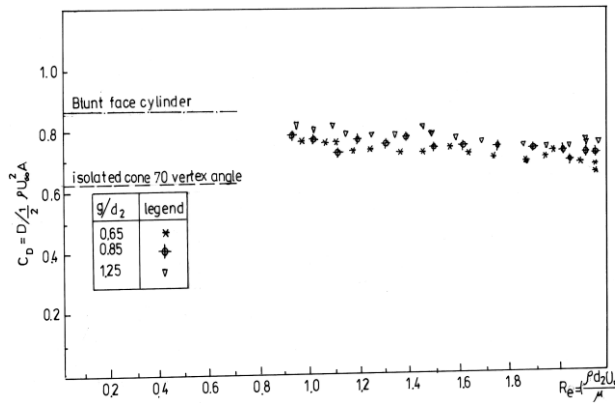


Fig.(7) Drag coefficient versus Reynolds number for a cone 70° vertex angle in tandem with the cylinder

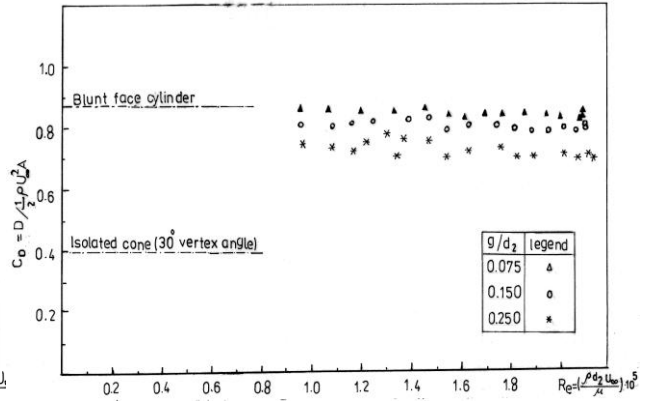


Fig.(10) Drag coefficient versus Reynolds number for a cone 30° vertex angle in tandem with the cylinder

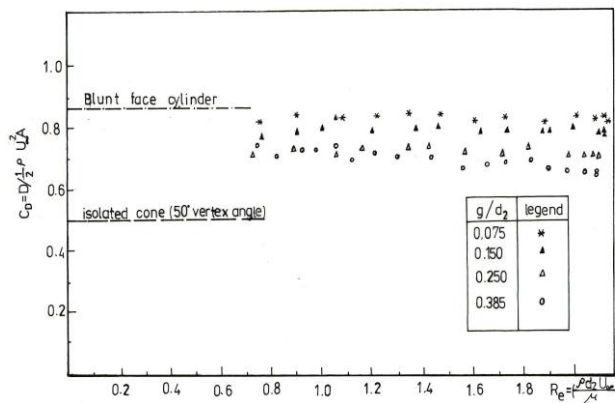


Fig.(8) Drag coefficient versus Reynolds number for a cone 50° vertex angle in tandem with the cylinder

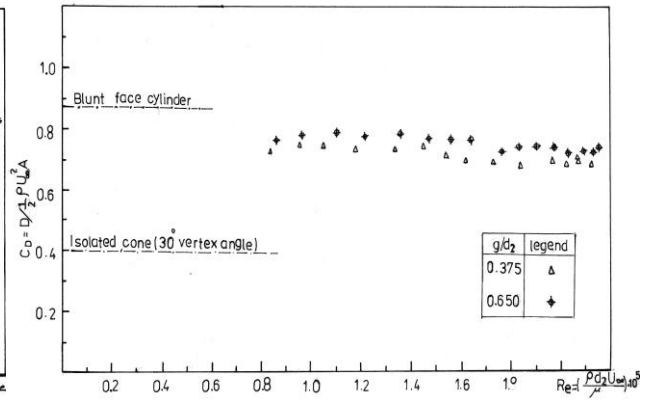


Fig.(11) Drag coefficient versus Reynolds number for a cone 30° vertex angle in tandem with the cylinder

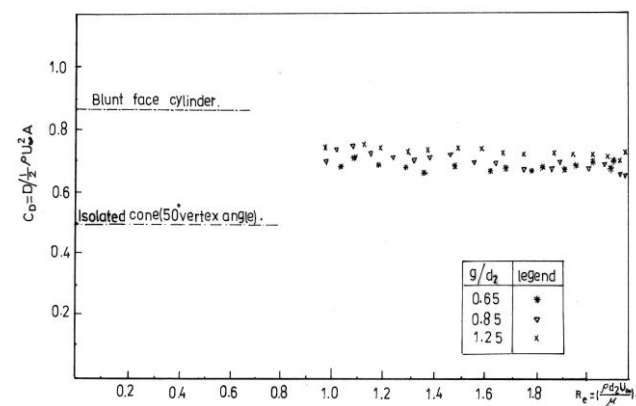


Fig.(9) Drag coefficient versus Reynolds number for a cone 50° vertex angle in tandem with the cylinder

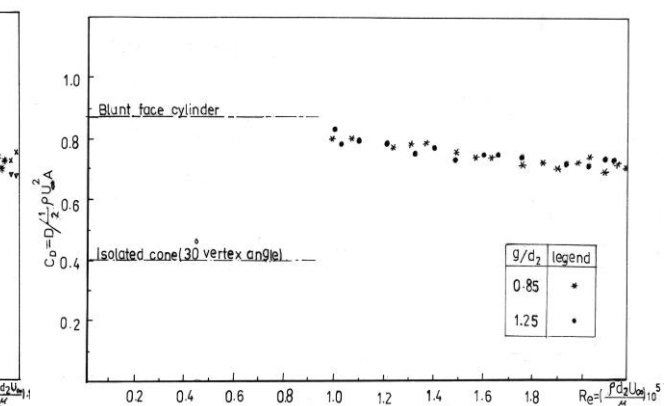


Fig.(12) Drag coefficient versus Reynolds number for a cone 30° vertex angle in tandem with the cylinder

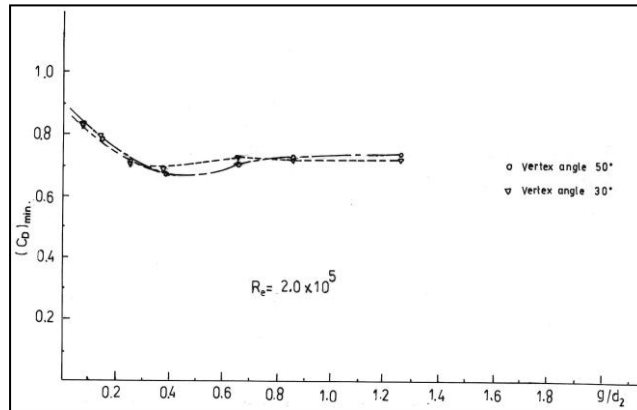


Fig. (13) Drag coefficient for the combination of cones tandem with the cylinder at various gap ratios

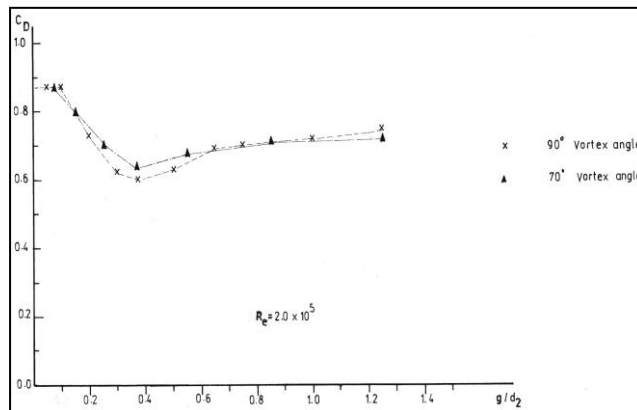


Fig.(14) Drag coefficient for the combination of cones in tandem with the cylinder at various gap ratios

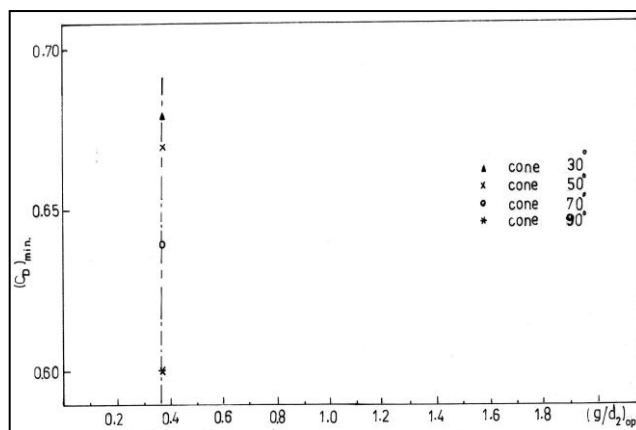


Fig.(15) Minimum drag coefficient various optimum gap ratio for the combination of cones in tandem with the cylinder.

